ChemistrySelect

Research Article
doi.org/10.1002/slct.202504136

Chemistry Europe
European Chemical Societies Publishing

www.chemistryselect.org

Synthesis, Characterization, Molecular Docking, and Biological Studies of Novel Quinoline – Schiff Base Ligand as Antibacterial and Anticancer Agents

V Geethalakshmi,[a] R Jayaprakash,[b] and K Umapathi*[c]

Emergence of new diseases and antimicrobial resistance, remain the driving forces behind the search for novel, biologically efficient, rapidly synthesizable, drugs. Recently, coordination compounds have gained attention because of their versatile biological properties. In this study, a new Schiff base compound named 3-Methoxy-2-(quinolin-3-ylimino)methyl phenol (MQIP) was synthesized through the condensation of o-vanillin with 3-amino quinoline. The formation of MQIP was confirmed using various analytical techniques such as ^{1}H-NMR, ^{13}C-NMR, UV-Vis, and FT-IR spectroscopy. Theoretical studies confirmed its drug-like characteristics. Molecular docking analysis against the selected protein (8GJ9), revealed good protein-binding potential with scores ranging from −6.7 to −9.9 kcal/mol, without violating any drug-likeness rules. Experimental evaluations further established its strong antimicrobial, antioxidant, and anticancer activities. The compound showed a minimum inhibitory concentration (MIC) of 12.5 µg/mL and inhibition zones of 20.5 mm, 20.4 mm, 21.6 mm against S. aureus, E. coli, and P. aeruginosa respectively. It also displayed antioxidant activity with an IC_{50} value of 139.83 ± 0.35 µg/mL, and anticancer potential against MCF-7 breast cancer cells with an IC_{50} value of 80 ± 0.25 µg/mL. Overall, both experimental and theoretical results indicate that MQIP is a promising drug intermediate with strong antimicrobial and anticancer properties.

1. Introduction

Pharmaceutical industry is always on the search for novel, biologically active, rapidly synthesizable intermediate compounds that can be easily coordinated to form complex drug molecules.[1] Schiff bases are one such intermediate compounds that are well known in coordination chemistry.[2] Schiff bases are formed by the condensation of amines (either aliphatic or aromatic) and carbonyl compounds (aldehydes or ketones). This results in the replacement of (C═O) bond by (–C═N–) azomethine group.[3] Schiff bases are excellent ligands and form metal complexes with transition metals and lanthanides inherent to their tuneable stereo-electronic structures.[4] Especially, Schiff bases that have a nucleophilic group like -SH, -NH_2, or –OH in the ortho-position to azomethine group have biological activity and excellent ligand characteristics.[5] Distinct Schiff bases are proven to selectively sense human serum albumin, bind with DNA, showcase antitumor as well as antibacterial activities in numerous research literatures.[6–8] These prophecies enable the use of Schiff bases and its derivatives for numerous therapeutic applications.

Quinoline, otherwise known as benzopyridine is a heterocyclic derivative containing nitrogen atom. Being a heterocyclic compound, it exhibits structural diversity as well as biological activity and is frequently investigated for deriving pharmaceutical drugs.[9] Quinoline demonstrates strong antibacterial, antiproliferative, antimalarial, anticonvulsant, anti-inflammatory, and other properties.[10–12] Schiff bases derived from Chitosan-Quinoline were demonstrated to have potential antibacterial, antioxidant, and antidiabetic activities.[13] Claimed to be an anticancer drug, quinoline derivative works by reducing angiogenesis, arresting cell cycles, disrupting cell migration and causing cell death. Research on quinoline-Schiff base metal complexes and their anti-microbial and anticancer properties has been documented in the literatures.[14,15]

Ortho vanillin (o-vanillin) are phenolic aldehydes obtained from orchid *Vanilla planifolia* and are frequently used in pharmaceuticals inherent to its antimicrobial and antioxidant activities.[16] Schiff bases synthesized by condensing 2-amino-4-chlorophenol with o-vanillin and its metal complexes were demonstrated to possess excellent antibacterial potentials.[17] In addition, Schiff bases ligand synthesized using *o*-Vanillin and *N*-phenyl-*o*-phenylenediamine and their metal complexes were demonstrated to have antibacterial, antioxidant. Further, their ability to bind with calf-thymus DNA and bovine serum albumin (BSA) were studied which demonstrated their anticancer abilities.[18] Similarly, Schiff bases derived from ortho-vanillin and 2-(2-aminomethyl)pyridine and its mononuclear uranyl complex were derived and characterized for various properties.[19] There are numerous studies that highlight the biological activities of o-vanillin and its derivatives.[20]

[a] *V Geethalakshmi*
Department of Chemistry, KIT-Kalaignar Karunanidhi Institute of Technology, Coimbatore, Tamilnadu 641402,, India

[b] *R Jayaprakash*
Department of Chemistry, School of Arts and Science, Vinayaka Mission's Chennai Campus, Vinayaka Mission's Research Foundation (Deemed to be University), Paiyanoor, Chennai 603104, India

[c] *K Umapathi*
Department of Biomedical Engineering, KIT-Kalaignar Karunanidhi Institute of Technology, Coimbatore, Tamilnadu 641402, India
E-mail: umapathi.uit@gmail.com

Computational methods provide low cost, chemical free and faster route for drug discovery and active molecule identification. These methods aid in studying the length and breadth of drug developments. Some notable use of theoretical methods includes, (i) quantitative structure–activity relationship (QSAR) calculation – for example density functional theory (DFT) computations and HOMO and LUMO (Highest Occupied Molecular Orbital and Lowest Unoccupied Molecular Orbital) characteristics are used for finding various QSAR parameters,[21–23] (ii) ADMET characteristics, Pharmacokinetics, drug-likeness scores of synthetic compounds can be found from theoretical tools,[24] (iii) binding affinity of synthesized molecules which directly reveal their molecules target identification capability can be determined by docking studies – software and servers that include such functions include, drug discovery workbench, Molegro, MOE, FlexX, and Autodock.[25–27]

With this brief introduction to the significance behind deriving novel Schiff base derivatives, properties of Quinoline, o-vanillin derivatives, and the benefits of using theoretical computation tools, the objectives of this work are:

- To synthesize a novel Schiff base ligand by condensation of quinoline with ortho vanillin and to conduct characterization studies using UV spectra, FTIR, H-NMR, and C-NMR.
- To conduct QSAR studies and molecular docking studies on the derived Schiff base ligand for predicting its drug likeness and protein binding characteristics.
- To conduct biological studies to verify the ligands antibacterial, antioxidant, and anticancer activities by agar-well diffusion, DPPH assay and MTT assay respectively.
- To compare the properties of the synthesized ligand with those in literature.

2. Materials and Methods

2.1. Materials Used

All chemical used in this research were from Sigma Aldrich, India and these chemicals were used as such without any modification for the synthesis and biological assays. Gram-positive bacteria, *Staphylococcus aureus* (MTCC 1430), and two gram-negative bacteria *Escherichia coli* (MTCC 1610) and *Pseudomonas aurogi-nosa* (MTCC 2453) are among the antibiotic-resistant pathogens obtained from MTCC (Microbial Type Culture Collection, India). And MCF7 breast cancer cell lines used for MTT assay were provided by NCCS (National Centre for Cell Sciences, Pune, India). Minimum Essential Media (MEM) without glutamine was used for cell growth.

2.2. Characterization Studies

The synthesized materials are dissolved in ethanol and their absorbance (in the range from 200 nm to 800 nm) is measured using Shimadzu UV-visible spectrophotometer, maintaining a scanning speeds between 4000 and 0.5 nm/min. Fourier transform infrared spectra (FTIR) of the synthesized materials are recorded by measuring % transmittance in 400–4000 cm^{-1} frequency range, adapting a KBr pellet method with IR affinity single reflection ATR spectrophotometer. These measurements are taken at room temperature using 64 scans at a spectral resolution of 2 cm^{-1}. An electrospray ionization mass spectrometry (ESI-MS) is used for recording the mass spectra of the synthesized ligand. Further, Bruker Advance III 500 MHz equipment is used to record nuclear magnetic resonance (NMR) spectra. The ^{1}H (proton) NMR and ^{13}C (carbon) NMR spectra of the Schiff base ligand are noted using DMSO-*d*6 solvent.

2.3. Computational Studies

All computational studies are conducted in HP, Elite Book operating on 64-bit, Intel Core i5-3320 M CPU at 2.60 GHz, with 8.00 GB RAM. Quantitative structure-activity relation (QSAR) parameters of the derived compound are predicted using online servers such as Molsoft and Molinspiration by submitting Simplified Molecular Input Line Entry System-(SMILES) notation of synthesized compounds. The derived compound parameters are verified with Lipinski's five rules. density functional theory (DFT) calculations are made for determining the chemical reactivity parameters. The HOMO-LUMO map and electrostatic potential map are obtained from DFT analysis conducted using Spartan -14 software. Using DFT results, E_{LUMO}, E_{HOMO}, global Hardness(h), softness(S), global Softness(s), chemical potential(μ), and global Electrophilicity(ω) are calculated.[28,29] Further, the molecule structure is then converted to mol2 file for docking purpose.

Docking studies aid in identifying the biomolecular interaction and thus, facilitate determining the drug efficacy in targeting and binding with protein. Cancerous cell growth related proteins such as 1Q2F (Cytotoxic to Cancer Cells), 2LEO (Esophageal cancer-related gene 2), 2N8B (cancer recognition site), 2N8C (cancer recognition site), and 8GJ9 (RAD51C N-terminal domain) are procured from protein data bank webserver and the obtained structures are verified with the help of online UCLA-DOE LAB-SAVES v6.1 pro-check server (https://saves.mbi.ucla.edu/). This study verifies the binding ability of the synthesized Schiff base ligand to five different proteins related to cancer. They are, (i) protein PDB-1Q2F which is a peptide from MDM-2 binding domain of P53 protein and is selectively cytotoxic to cancer cells; It belongs to a tumor suppressor P53 fragment, (ii) 2N8B & 2N8C which are cancer recognition site proteins, (iii) 8GJ9 – which belong to RAD51C N-terminal domain; this represents a DNA binding protein, (iv) 2LEO which is Esophageal cancer-related gene 2. Ramachandran plots are drawn and used for verifying protein structures. Then active site identification is carried out by online webserver, (http://www.scfbio-iitd.res.in/dock/ActiveSite.jsp) developed by IIT, Delhi, India and efficient docking sites are recorded. Using the recorded data, initial online docking is conducted through Swiss dock (https://www.swissdock.ch/) and the server produced best interactions are downloaded and used for the further offline docking. Offline docking is conducted in

MOE 2015 for the downloaded online best score PDB files. The interactions are calculated and compared with the online results.

2.4. Biological Studies

Biological assays are the conventional methods adapted for validating a materials' bioactivity. This work utilizes them as a validation tool for confirming the theoretical results obtained from computational methods.

2.4.1. Antibacterial Assay

Antibacterial activity of the synthesized compound is tested adapting agar well diffusion method.[30] The assay protocol starts with spreading a known volume of the microbial culture across the agar plate surface, followed by creating circles of 6 mm diameter with aseptic tip. Then in each circle varying concentrations of the synthesized compound is added and incubated. Standard ciprofloxacin of 10 µg/mL is used as control. After incubation, growth inhibition was measured in millimetre. The minimum inhibitory concentration and maximum zone of inhibition are recorded. The statistical standard deviation (SD) was calculated from the trial results.

2.4.2. Antioxidant assay

Antioxidant activity of the synthesized compound is tested by determining its free Radical Scavenging Activity commonly known as RASA. This assay is conducted by using different stable free radicals like, (i) (2,2-Diphenyl-1-picrylhydrazyl) – DPPH, (ii) (2,2′-azino-bis(3-ethylbenzothiazoline-6-sulfonic acid)) – ABTS or (iii) Superoxide, (iv) Ferric Reducing Antioxidant Powder (FRAP).[31] Superoxide is a free radical generated naturally by body and thus, superoxide antioxidant assays could reveal the efficacy of the synthesized compounds in neutralizing the naturally produced ROS.[32] ABTS is blue-green in color and addition of antioxidants decolorises it.[13] DPPH is deep purple in color and addition of antioxidants changes its color to yellow. FRAP is also a colorimetric assay which measures the antioxidant activity of a sample by assessing its ability to reduce ferric to ferrous ions.[33] The present study utilises DPPH assay to quantify the antioxidant potential of the synthesized Schiff base compound. DPPH assay protocol starts with the preparation of DPPH stock solution by dissolving 24 mg of DPPH in 100 ml of methanol. Now, about 3 mL of DPPH solution is mixed with 12.5, 25, 50, 100, and 200 ppm of synthesized compound in test tubes. A standard containing 3 mL DPPH in 100 mL methanol is taken. Then the test tubes were kept under darkness for 30 min. Following this, absorbance at 517 nm is determined [25] and percentage antioxidant activity is calculated using the below formula:

$$Percentage\ antioxidant\ activity = \frac{ABS_C - ABS_{TS}}{ABS_c}$$

where ABS_C represents absorbance in control and ABS_T represents absorbance in test specimen.

2.4.3. Anticancer studies

Anticancer activity of the synthesized compound is tested by determining its cell viability against MCF7 cancer cell line, by adapting MTT (3-(4,5-dimethylthiazol-2-yl)-2,5-diphenyltetrazolium bromide) assay.[7,22] The assay protocol starts with culturing MCF7 cell in 96-well plate by incubating it overnight. Now varying concentrations of synthesized compound are added with the cultured cells and the same is incubated at 37 °C maintaining 85% humidity and 5% CO_2 for 48 h. After incubation, well-plate containing both treated cell and control is washed with fresh medium (200 µL). Now, MTT solution of (0.5 mg/mL) is added to the assay plate and the same is incubated for 3 h. Finally, the purple formazan crystals formed are solubilized by adding 200 µL of DMSO per well and ELISA microplate reader is used to determine optical density (OD) at 590 nm. From OD measurements for treated cells and control cells, percentage cell viability is calculated using the below formula

$$\text{Percentage cell viability} = \frac{\text{Optical Density}_{\text{Test Cell}}}{\text{Optical Density}_{\text{Control}}} \times 100$$

The bioactivity of the compounds is compared with docking results to validate their efficacy. The IC_{50} value which is the most commonly used measure for quantifying biological activity of a compound is determined. IC_{50} refers to the concentration of the synthesized compound that brings in 50% cell viability in MTT assay.

2.4.4. Statistical analysis

The antimicrobial assay results are expressed in terms of mean and SD obtained for the experimental results. The SD calculator available online at: https://www.calculator.net/standard-deviation-calculator.html is used for obtaining the SD values. Further, regression analysis is conducted to find the IC_{50} values in the case of antioxidant assay and MTT cell viability assay. Quest Graph IC_{50} Calculator available online at: https://www.aatbio.com/tools/ic50-calculator is used for obtaining IC_{50} values.

3. Synthesis of Quinoline Schiff Base

3.1. Synthesis of 3-Methoxy-2-(quinolin-3-ylimino) methyl phenol (MQIP)

The light-yellow coloured Schiff base MQIP organic compound is synthesized by the condensation of 3-amino quinoline with o-vanillin. Ortho vanillin (0.05 mol) was dissolved in 100 mL ethanol followed by dropwise addition of 3-amino quinoline (0.05 mol). The mixture was heated under reflux for 5 hours. Light-yellow precipitate formed after reaction completion is filtered and dried under vacuum at 50 °C. About 11.4 gm (82%) of organic compound MQIP is obtained from the process. The chemical reaction representing the formation of MQIP complex is shown in Figure 1.

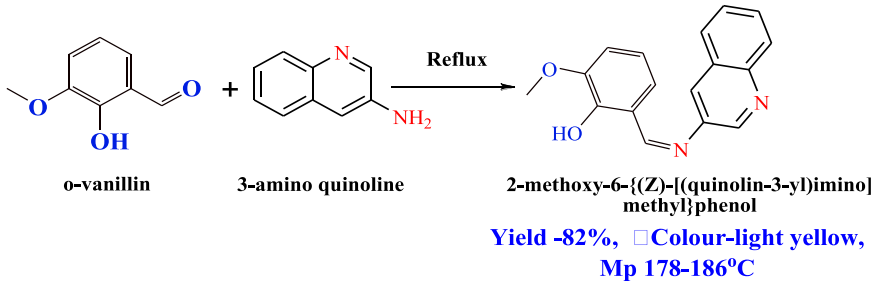

Figure 1. Preparation scheme of MQIP.

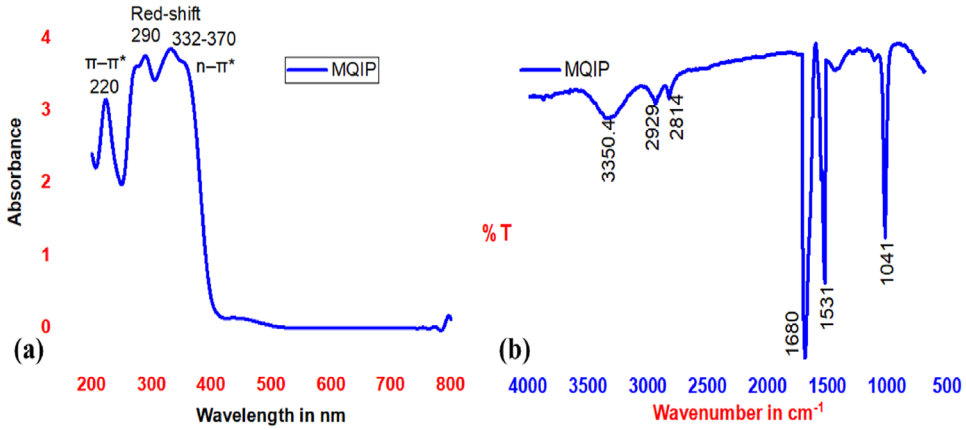

Figure 2. a) UV Absorption spectra and b) FTIR spectra of MQIP.

4. Results and Discussion

This research successfully prepared the heterocyclic quinoline ring with pharmacological active imine and hydroxy group containing Schiff base MQIP. The isolated compound is confirmed by known spectral techniques.

4.1. Characterization results of MQIP

The UV absorption spectrum of Schiff base MQIP is recorded by dissolving MQIP in ethanol and measuring absorbance in the range from 200 nm to 800 nm and the results are depicted in Figure 2 a for analysis. The tetra dentate 3-Methoxy-2-((quinolin-3-ylimino) methyl) phenol Schiff base MQIP exhibits n→π* and $\pi \rightarrow \pi$* transition at 332–370 nm and 290 nm. The 1st transition at 290 nm represents the $\pi \rightarrow \pi$* transition corresponds to the heterocyclic moiety while the second transition band between 332–370 nm represents the n→π* transition corresponding to azomethine (–C═N–) group of Schiff base. The electronic absorption spectra pattern almost coincidence with that in literature though there is slight deviation due to methoxy group.[34]

Next to UV absorption spectra, FTIR vibrational spectra are obtained using KBr pellet method and the obtained spectra is depicted in Figure 2b. FTIR spectra of MQIP reveals six notable peaks. The slightly broad absorption band with peak centred around ~3350.4 cm^{-1} corresponds to the phenolic –OH. The intensity of this peak reduced in comparison to the original ortho vanillin.[16] This weak IR absorption is due to the formation of strong intramolecular hydrogen bond between the phenolic oxygen and imine nitrogen in the synthesized Schiff base. This internal hydrogen bond weakens the O–H bond, making it less polar and reduces its ability to absorb IR light.[35] Weak absorption between 2929 cm^{-1} and 2814 cm^{-1} is due to the aromatic C–H stretching vibrations.[16] The sharp peak at 1680 cm^{-1} is due to the C═N stretching band resulting from the imine bond.[2] Another sharp peak at 1531 cm^{-1} corresponds to C═C which confirms the presence of benzene ring.[36] While the peak absorption at 1041 cm^{-1} corresponds to C–O vibrations corresponding to carbonyl group.[3]

The proton and carbon NMR results are obtained for MQIP and its metal complexes to further confirm its constituents. Figure 3a represents the integrated full spectrum of MQIP and inset images in Figure 3b–d, represent the expanded spectral data corresponding to its individual constituents. Spectral peak at 9.89 ppm corresponds to the free phenolic -OH proton and is represented by Figure 3b. Azomethine (–C═N) proton corresponding to quinoline Schiff base appears at 8.69 ppm which is given by Figure 3c. While the aliphatic methoxy group proton of o-vanillin moiety is observed at 3.83 ppm (Figure 3d). Multiplets corresponding to quinoline protons are (i) doublet H(2) at 8.13 – 8.12 ppm, (ii) H(4) at 8.04 – 7.98 ppm, (iii) H(7) at 7.72 – 7.69, (iv) H(6) at 7.63 – 7.60 ppm, (v) H(8) at 7.43 – 7.41 ppm. Multiplets corresponding to o-vanillin appeared at (i) H(2) at 6.96 – 6.94 ppm.

The ^{13}C NMR spectra results of MQIP is depicted in Figure 4. The spectra showed a peak at 163.18 ppm which corresponds

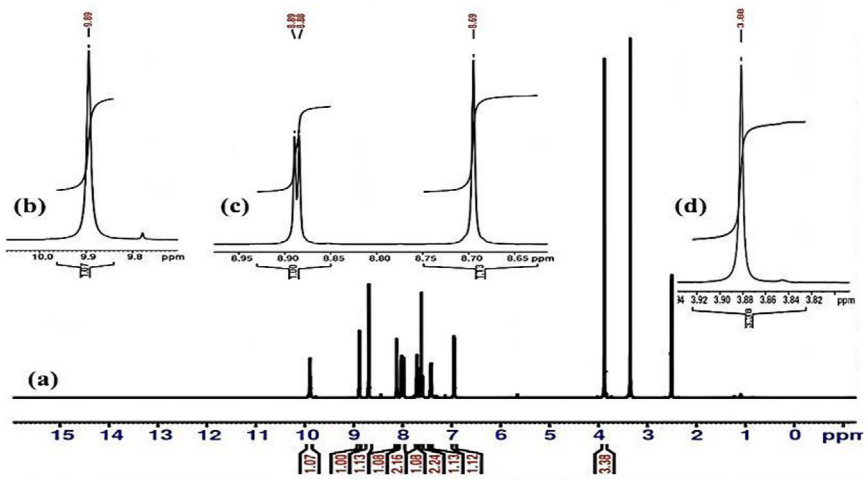

Figure 3. a) [1]H-NMR spectrum of MQIP, b) Phenolic – OH single peak expansion, c) azomethine (–C═N–) expansion between 8.65 – 8.89 ppm, and d) Methoxy group proton peak.

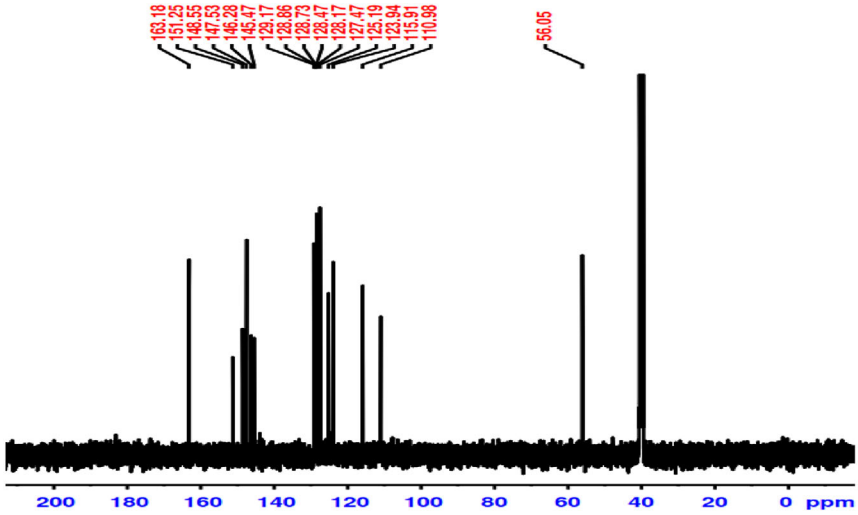

Figure 4. [13]C NMR spectrum of MQIP.

to C═N carbon. The aromatic carbon atoms appeared between 115.91 ppm and 129.17 ppm of quinoline moiety. The peaks corresponding to methoxy group, methyl carbon is noticed at 56.05 ppm. The [13]C NMR spectra obtained coincides with the reported values in literature.[37,38] Both NMR spectra have confirmed the derived organic compound MQIP.

4.1.1. NMR Results

[1]H NMR (500 MHz, DMSO-*d6*) δ 1H NMR (500 MHz, DMSO-*d6*) δ 9.89 (s, 1H), 8.89–8.88 (d, J = 5 Hz, 1H), 8.69 (s, 1H), 8.13–8.12 (t, J = 5 Hz, 1H), 8.04 – 7.98 (dd, J = 7.3, 1.5 Hz, 2H), 7.72 – 7.69 (m, 1H), 7.63 – 7.60 (m, 2H), 7.43–7.41 (dd, 1H), 6.96 – 6.94 (d, J = 10 Hz 1H), 3.83 (s, 3H). [13]C NMR (125 MHz, DMSO-*d6*) δ 163.18, 151.25, 148.55, 147.53, 146.28, 145.47, 129.17, 128.86, 128.73, 128.47, 128.17, 127.47, 125.19, 123.94, 115.91, 110.98, 56.05

The synthesized Schiff base ligand has a syn-orientation that is the phenolic O–H and imine nitrogen lie on the same side, stabilized by an intramolecular hydrogen bond. Both the NMR spectrum and FTIR results support this syn-orientation of MQIP ligand. For instance, considering [1]H NMR spectrum (DMSO-d_6), the phenolic O–H signal appears as a singlet at δ 9.89 ppm and azomethine proton appears at δ 8.69 ppm. Persistence of these signals in DMSO-a solvent that weakens hydrogen bonding and its downfield shift, confirms a strong intramolecular O–H… N interaction that favours syn-orientation. Further, there is a single set of azomethine and phenolic resonances, indicating a single dominant isomer in solution, which is syn form in the case of ortho-hydroxy imines. Considering FTIR spectra, the OH stretch is reduced in intensity and shifted towards low frequency ~3350 cm^{-1} instead of near 3600 cm^{-1}, which confirms the presence of a strong intramolecular hydrogen bond, further supporting the syn-orientation of the synthesized ligand. These spectral data provide strong and cohesive proof that MQIP adopts the syn-oriented, intramolecularly H-bonded enol-imine form in solution. Further, the mass spectrometry results of the synthesized MQIP ligand revealed molecular ion peak at mass-to-charge ratio (m/z) (main peaks, ESI^+) = 279 $[M + H]^+$, 301

Table 1. Online Molsoft QSAR parameters

Si. No.	Molsoft parameters	Values
1	Mol. Formula	C_{17} H_{14} N_2 O_2
2	Mol. Weight	278.11
3	HBA*	4
4	HBD*	1
5	LogP	~(3.2–3.4)
6	LogS (moles/L)	−3.16
7	PSA (A^2)	40.33
8	Vol(A^3)	265.6
9	Drug- likeness	−0.58
10	Blood Brain Barrier	4.82

$[M + Na]^+$, 557 $[2\ M + H]^+$. Whereas, the calculated molecular weight of the ligand ($C_{17}H_{14}N_2O_2$) is 278.11 amu. The major molecular ions were $[M + H]^+ \approx 279$ amu and there is no fragmentation observed below 250 amu. These results support the successful synthesis of Schiff base and further, coincide with those reported in literatures.[39–41]

4.2. Theoretical Studies on MQIP

4.2.1. QSAR analysis

Molsoft analysis: SMILE notation of the synthesized compound is created from its geometrical structure using Chemsketch tool. These SMILE notations are submitted to Molsoft server and QSAR parameters are found, and the same is presented in Table 1. As per Lipinski's rule of five, molecular weight, logP, polar surface area, H-bond donors obtained by summing NH and OH, and H-bond acceptors given by sum of N and O values are calculated and related to MQIP's drug characteristics.[42] It is found that MQIP ($C_{17}H_{14}N_2O_2$) has one hydrogen-bond donor (HBD = 1) (the phenolic OH) and four hydrogen -bond acceptors (HBA = 4) (the imine-N, quinoline-N, phenolic O, and methoxy O). Further, its QSAR descriptors were, logP ≈ 3.2–3.4, moderate TPSA, single Lipinski violation for lipophilicity). These values support acceptable membrane permeability while retaining sufficient polarity for binding and solubility. In addition, volume, drug likeness and blood brain barrier score (BBBS) are also calculated. Figure 5 a presents the drug likeness graph.

Molinspiration analysis: A second validation of drug-likeness of the materials synthesized is carried out using Molinspiration software. The results obtained from Molinspiration analysis are presented in Table 2. Experimental results supported the Veber rule parameters and there were zero violations for the given compounds.[43,44] The compounds showed bioactivity score between −0.48 and 0.16 which lies in the moderate activity limit between −0.5 and 0. When compared to previously reported results,[45] the synthesized compounds showed better inhibition except for the case of kinase inhibitor. Though Molsoft and Molinspiration data are slightly different, both the results supported the drug-like behavior of the synthesized compounds.

Examining the drug-likeness score of MQIP reveals that it falls just below the neutral threshold (−0.58), which indicates, it may not have strong activity across all pharmacological targets in the Molinspiration database. Molinspiration bioactivity scores between −0.50 and 0.00 are moderately active — suggesting potential but not optimal activity against the modelled target classes (GPCR, kinase, enzyme inhibition, etc.). This interpretation is supported by literature results where it is concluded that Schiff-base derivatives with bioactivity scores between −0.70 and 0.00 still exhibited significant antibacterial and anticancer potential when other ADMET descriptors were favorable.[46] In the present case, MQIP retains the physicochemical properties within the drug-like space exhibiting, logP ≈ 3.2–3.4, molecular weight 278 Da, TPSA 41–55 $Å^2$, HBD = 1, HBA = 4, and only one Lipinski violation (logP). These descriptors support the fact that MQIP's score does not disqualify it as a potential lead compound; but places it in the "moderately promising" category, making it suitable for further optimization (e.g., substitution on the quinoline ring or imine stabilization) to improve binding affinity and potency.

DFT computation: DFT computations for the molecular structures carried out using Spartan-14 and the parameters like HOMO and LUMO gaps, electrostatic potential map is derived. It is found that MQIP had a E_{HOMO} value = −8 eV, and E_{LUMO} = 2.2 eV with a dipole moment of 7.61 Debye. Further, Koopan parameters such as global softness (S) = 0.098 eV, global hardness (η) = 5.1, electrophilicity (ω) = 0.82, Chemical potential (μ) = 2.9, and softness σ = 0.196 are obtained from HOMO-LUMO values. The electrostatic potential map, the HOMO-LUMO potential map are presented in Figure 5b and Figure 5c respectively. These values coordinate with the values in literature.[45,47] The electrostatic potential map (EPM) of MQIP is multi-colored which reveals the presence of both high- and low-density electrons in it. Molecular characteristics such as total charge distribution, chemical reactivity, electronegativity, dipole moment, lipophilicity can be derived from the EPM.[48] The dipole moment depicts the binding interactions between synthetic molecules and receptor proteins and lipophilicity depicts the capacity of chemicals to enter the lipophilic membrane of microbes. All QSAR predictions revealed moderate drug ability of MQIP. Once the QSAR predictions are made docking studies are conducted for the compounds.

QSAR of MQIP and Related Schiff Bases: MQIP ligand exhibits favorable drug-like properties with a molecular weight of 278 Da, logP ~3.2–3.4, and TPSA ~41–55 $Å^2$, meeting Lipinski's rules except for one logP violation. DFT computations reveal, a dipole moment of 7.6 D, $E_{HOMO} \approx -8$ eV, $E_{LUMO} \approx +2.2$ eV, and global hardness $\eta \approx 5.1$, which suggests moderately reactive and electronically stable scaffold. Further, the presence of ortho hydroxy and azomethine groups stabilizes the syn-form, providing donor sites for metal chelation, enabling enhanced activity metal complexes to form.

QSAR Trends in Related Compounds: O-vanillin and quinoline-derived Schiff bases reported in recent literatures reveal that, (i) electron donating groups like methoxy are responsible for enhancing HOMO energy and antioxidant activity, (ii) planarity improves DNA binding and thus its docking

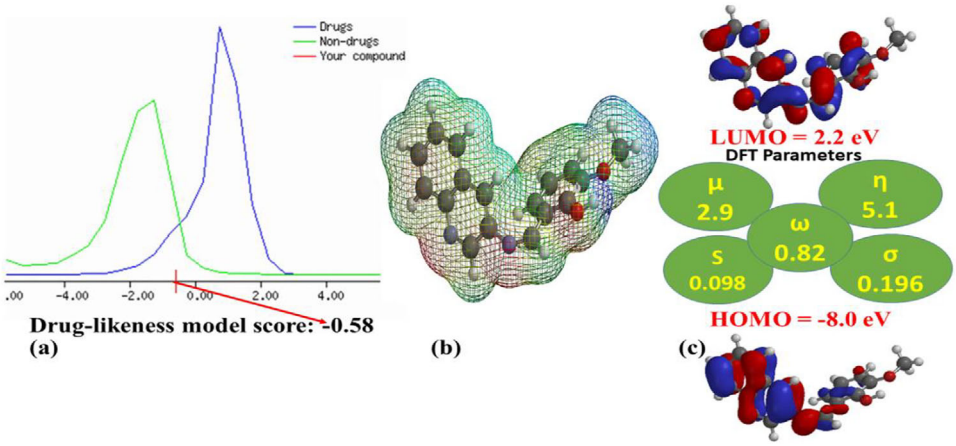

Figure 5. a) Online Molsoft drug-likeness graph, b) Electrostatic potential map, and c) Spartan 14 DFT Koopman parameters with HOMO and LUMO energy orbitals of MQIP.

Table 2. Molinspiration theoretical QSAR parameters.

Si. No.	Molecular descriptors	Values	Si. No.	Bioactivity predictors	Values
1	No of atoms	21	1	GPCR ligand	−0.35
2	MW	278.31	2	Nuclear receptor ligand	−0.41
3	nrotb	3	3	Kinase inhibitor	0.16
4	nON	4	4	Protease inhibitor	−0.04
5	miLogP	3.17	5	Ion channel modulator	−0.48
6	nOHNH	1			
7	TPSA	54.72			
8	Vol(A^3)	252.11			
9	No. of violations	0			

to protein sites, (iii) Intramolecular O–H···N hydrogen bonding increases metal-binding ability and overall bioactivity. 3D-QSAR and docking studies reveal that bioactivity of Schiff bases results from moderate lipophilicity (logP 2–4), well-placed hydrogen-bond donors/acceptors, and extended π-surface for protein pocket and DNA interactions. MQIP correlates well with these criteria which confirms its biological effect is driven by $\pi-\pi$ stacking, redox modulation, and metal-mediated mechanisms.

Implications and Design Recommendations: QSAR guided optimization of MQIP properties focus on modifying electronic properties and metabolic stability in spite of preserving donor functionality and planarity. Possible modifications include, (i) quinoline substitution – by C6 halogenation or N1 lipophilic substituents, in order to enhance cell penetration, (ii) stabilization of the imine bond which improves its in vivo half-life, (ii) Metal complexation, to shift electronic parameters (lowering C═N frequency, altering HOMO/LUMO gap) which significantly enhances cytotoxic activity, making metal–ligand derivatives promising anticancer leads. For improving antibacterial potency mimicking fluoroquinolones, 3-carboxy-4-oxo pharmacophore and other fluoroquinolone-like substituents are introduced for transforming the scaffold similar to a conventional gyrase inhibitor chemotype.

Table 3. Procheck save.6.1 server outcomes of cancer related proteins.

Parameters	1Q2F	2LEO	2N8B	2N8C	8GJ9
Residue properties	Pass	Pass	Pass	Pass	Pass
Bond len/angle	Pass	Pass	Pass	Pass	Pass
Planar groups	Pass	Pass	Pass	Pass	Pass
Residues in favoured region %	96.6	100	92.9	100	99.4

4.2.2. Molecular Docking Studies

Procheck Analysis: Procheck results in the form of Ramachandran plot reveals the distribution of torsion angles in a protein. It provides the rotations of polypeptide chain that are not allowed as they result in steric hinderance resulting from collision of atoms. These plots serve in selecting the allowable protein structures in terms of dihedral angles Ψ versus Φ. All proteins were uploaded one by one and verified. The obtained Ramachandran plots are interpreted and the allowed and disallowed regions are noted. The interpreted outcomes are presented in Table 3. All proteins favoured regions exist between 92.4% and 100%.

Ramachandran plots were downloaded from Procheck save 6 servers and model of 2LEO is shown in Figure 6. The yellow-

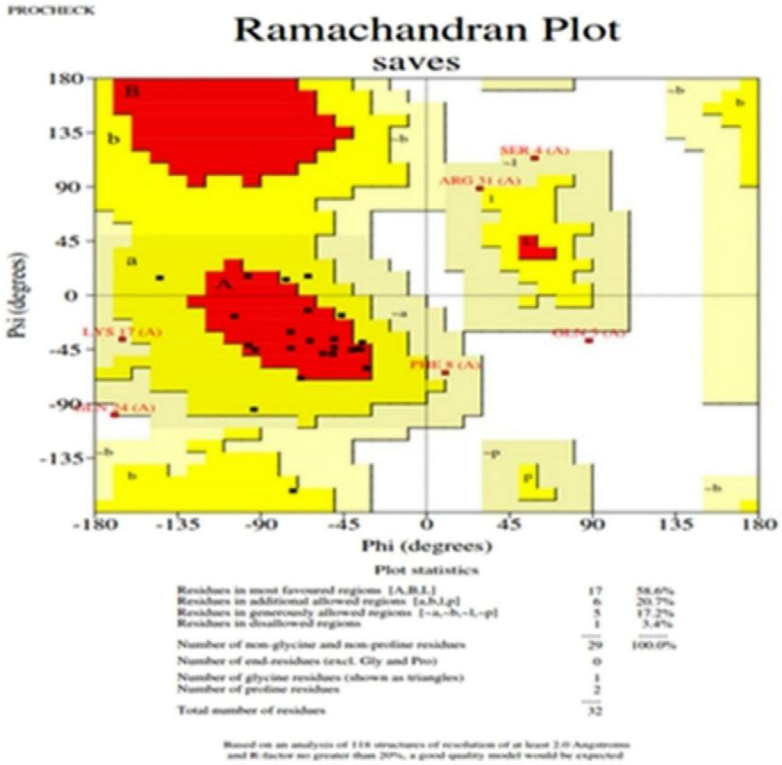

Figure 6. Pro-check online Ramachandran plot of cancer related protein 2LEO.

Table 4. Online cavity docking results of Swiss dock.

PDB ID	JOB ID	Cavity point			Volume of the cavity
		X	Y	Z	
1Q2F	60,718,369	−1.695	7.932	−1.728	1707
2LEO	25,523,169	−7.493	−9.252	16.010	1890
2N8B	64,819,006	6.095	−7.347	−2.976	792
2N8C	43,318,385	−11.141	−17.095	−5.230	855
8GJ9	87,945,785	18.838	11.069	45.398	1699

colored regions are termed the allowed regions and grey represents the not allowed regions in the plot. The verified proteins are taken for docking with QSAR properties verified MQIP compound for theoretical evaluation.

4.3. Active Site Prediction

Active site in the selected proteins that directly reveal the cavity points in uploaded proteins that can dock the synthesized structures are identified using online server, "https://scfbio-iitd.res.in/dock/activesite.jsp". And the active cavity point is measured and recorded. The obtained results are presented along with the protein volume and job ID in Table 4. below

4.4. Swiss Dock Analysis

Docking analysis of the synthesized compound is carried out by providing user-defined cavity points obtained from active site prediction results. Once the required input files were fixed, solvents, and water molecules were removed and hydrogen atoms were added. Ionization state of N-and C-terminal were fixed. The verified proteins are uploaded for determining the binding ability measurement at specified (user defined) active sites. The cavity volume and the docking size with scores against the selected cancer target proteins are presented in Table 5.

Online Swiss dock results reveal that the compound an Autodock Vina score between (−82.3) and (−98.6) kcal/mol for all the proteins except 8GJ9 (−6.7 kcal/mol). After completion, the best docking score pose is opened and downloaded. Digital images of the downloaded poses of various selected proteins are presented in Figure 7a–e. Similarly, the 2D ligand interactions are viewed by opening 3D docking images with MOE docking software. Digital images of 2D interaction of MQIP against various proteins is shown in Figure 7f–j. Due to multiple chains and based on volume more similar amino acids are observed in all docking outcomes.

4.5. Offline Docking

After the interpretation of online docking results, the downloaded best score PDB files are utilized for offline docking in MOE docking software. Both the ligand and receptor proteins containing PDB files imported to MOE software and docked. The five docking scores as produced by MOE tool are recorded and interpreted. The images of the same are shown in Figure 8. The docking reports are verified with online docking scores. Out of five docking scores, MQIP exhibited best docking score between

Table 5. Online Swiss dock server docking score and cavity outcomes of selected proteins.

PDB ID	Pocket ID	Best Vina docking score (kcal/mol)	Volume of cavity (A^3)	Centre (x, y, z)	Size of docking (x, y, z)
1Q2F	C1	−82.3	43	−7, 4, 4	21, 21, 21
2LEO	C3	−87.2	334	4, 9, 10	20, 20, 20
2N8B	C2	−98.6	37	−3, −8, −14	20, 20, 20
2N8C	C5	−90.9	3	4, −4, 2	20, 20, 20
8GJ9	C5	−6.7	85	10, 2, 53	20, 20, 20

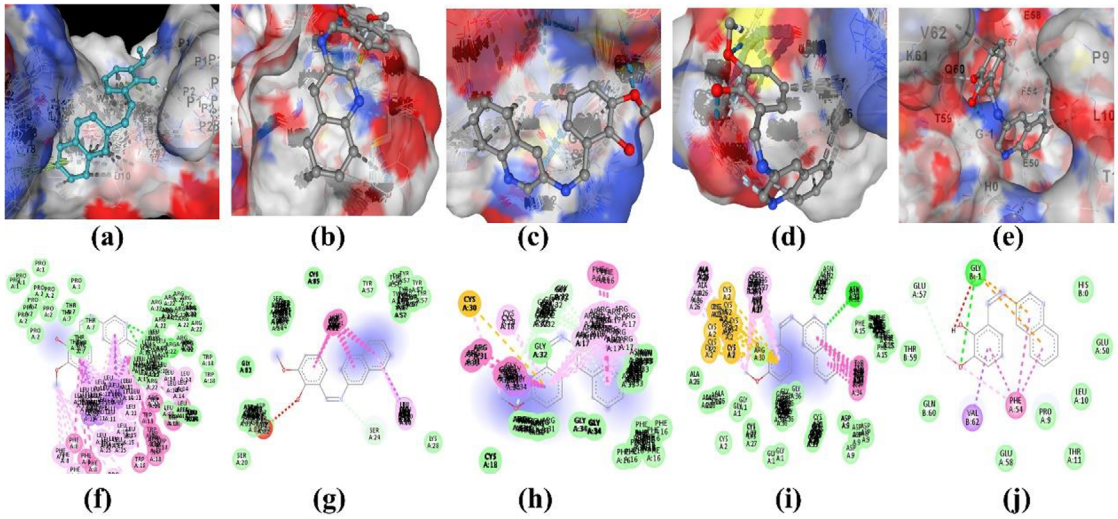

Figure 7. a) Docking interaction results of MQIP against the selected protein a) 1Q2F b) 2LEO c) 2N8C d) 2N8B and e) 8GJ9, 2D docking interaction of MQIP against the selected protein f) 1Q2F g) 2LEO h) 2N8C i) 2N8B and j) 8GJ9.

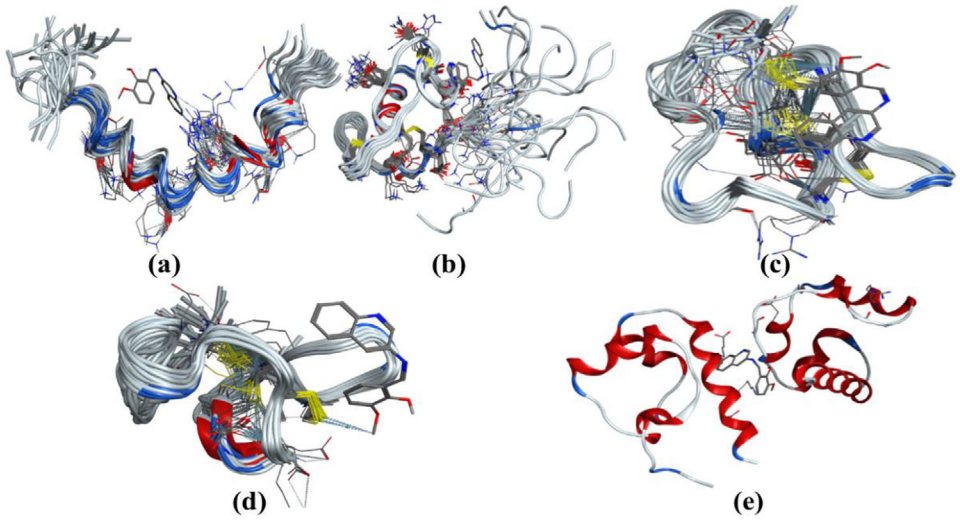

Figure 8. MOE docking interaction results of MQIP against the selected proteins a) 1Q2F, b) 2LEO, c) 2N8C, d) 2N8B, and e) 8GJ9.

−28.9 kcal/mol and −81.1 kcal/mol for all proteins except 8GJ9 (−5.3 kcal/mol). The offline results are almost coincidence with the online results.

This work observed online docking score in the order of 2N8B > 2N8C > 2LEO > 1Q2F > 8GJ9. But, offline MOE docking scores are in the order of 2LEO > 2N8B > 2N8C > 1Q2F > 8GJ9. The docking scores have revealed the anticancer binding ability of the synthesized compound. The next section of the article presents the biological evaluation to support the theoretical results.

Table 6. Antimicrobial agar well and micro dilution analysis results of MQIP.

Comp. ID	Name of the pathogens ZOI in mm/(MIC in µg/mL)		
	S. aureus	*E. coli*	*P. auroginosa*
MQIP (100 µg/Disc)	20.5 ± 1.22/ (12.5)	20.4 ± 2.02 /(12.5)	21.6 ± 0.65 /(12.5)
Ciprofloxacin (10 µg/Disc)	18 ± 1/ (2.5)	16 ± 1.5/ (2.5)	22 ± 1/ (5)

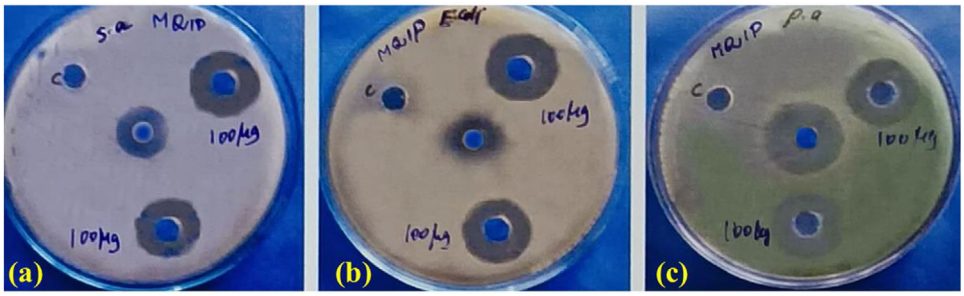

Figure 9. Antimicrobial agar well dilution method dual trial conducted microbial. plates of MQIP against a) *S. aureus*, b) *E. coli*, c) *P. auroginosa*.

4.6. Biological Studies on MQIP

Antibacterial activity: Antibacterial activity of MQIP is evaluated by using Agar-well diffusion assay. *S. aureus* a gram-positive bacterium, *E. coli and P. auroginosa* variants from gram negative bacteria are used for evaluating the antibacterial effectiveness of MQIP complex. Ciprofloxacin (10 µg/mL) is used as control [49,50] and the assay results obtained in terms of zone of inhibition (ZOI) are presented in Table 6. MQIP is a complex with imine group and heterocyclic compound in it. MQIP in different concentrations ranging from 5 µg/mL to 100 µg/mL (MQIP in DMSO) are used for testing the antibacterial efficacy of the synthesized compound. Assay results depict that a minimum inhibition concentration (MIC) of 12.5 µg/mL of MQIP is required for initiating bacterial inhibition. The ZoI measurements were recorded by for different concentrations of MQIP. It is found that MQIP inhibited *S. aureus, E. coli*, and *P. auroginosa* with a ZoI of 20.5 mm, 20.4 mm, 21.6 mm, respectively. MQIP compound exhibited a SD of 1.22, 2.02 and 0.65 mm respectively across the trials. While Ciprofloxacin showcased a SD value of 1.5, 1, and 1.5 mm respectively. These results reveal the antimicrobial efficacy of the complex compound. Digital images of the agar-well diffusion plates used for the assay are presented in Figure 9. The zone of inhibition and MIC values are almost coincidence with the reported quinoline based Schiff bases.[51,52]

It could be inferred from the assay results that MQIP shows a ZOI against both gram positive and gram-negative bacteria but, at 10-fold doses in comparison to Ciprofloxacin which indicates MQIP has a weaker and mechanistically distinct antibacterial action. This is due to the very reason that Ciprofloxacin and MQIP are fundamentally different chemotypes with distinct pharmacological implications resulting from their structural differences. This could be better understood from their structure activity relationships (SAR) which is detailed below.

Ciprofloxacin is a fluoroquinolone with a bicyclic 4-oxo-quinoline carboxylic acid scaffold. It is characterised by C3–COOH and C4═O pharmacophore. Specifically, it has (i) C6-fluorine that enhances degree of penetration to bacterial cells, (ii) piperazinyl group at the C7 position is a fundamental modification site that modulates spectrum, potency, and pharmacokinetics, (iii) N1 cyclopropyl group further increases potency by target inhibition. The 3-COOH/4-oxo motif of fluoroquinolones, chelate Mg^{2+} in the gyrase–DNA complex, which inhibits bacterial DNA gyrase and topoisomerase IV by canonical mechanism. However, MQIP is a quinoline Schiff base containing a conjugated quinoline–imine–aryl system, a phenolic OH and a methoxy substituent, with both the imine and quinoline nitrogen serving as donor sites. The phenolic OH and azomethine enables intramolecular H-bonding that, (i) stabilizes the syn enol-imine form and (ii) permits deprotonation and coordination to metals, which are important for anticancer effects. Whereas, Methoxy substitution contributes to moderate antioxidant activity ($IC_{50} \approx 139.8$ µg/mL). MQIP's planarity and donor set favours $\pi-\pi$ stacking, DNA intercalation, metal chelation, supporting strong docking scores against cancer-related proteins. Further, MQIP's ability to form (O,N)-bidentate metal complex enhances bioactivity. SAR analysis for ciprofloxacin confirms the necessity of 3-COOH/4-oxo and C6-F for potency and inhibition against bacterial DNA, while MQIP's SAR suggests that the phenolic OH and C═N are key contributors to bioactivity, with metal complexation further enhancing cytotoxicity to cancerous cells.

However, antimicrobial activity of MQIP ligand could be enhanced by suitable SAR-driven modifications to include, (i) quinoline substitution (C6 halogenation, N1 lipophilic groups) to enhance bacterial DNA penetration, (ii) imine stabilization to improve metabolic stability, and (iii) systematic variation of the o-vanillin ring electronics. Specifically, to get antimicrobial functions similar to ciprofloxacin, 3-carboxy-4-oxo pharmacophore and C6-F/C7-piperazinyl substituents would be required. Otherwise, MQIP ligand is a potential candidate for alternative mechanisms such as DNA interaction, ROS generation, and metal-mediated cytotoxicity which are promising for anticancer

Table 7. SAR-driven modifications for MQIP ligand.

No.	Analogue ID	Structural change from MQIP 3-MeO-2-((quinolin-3-ylimino)methyl)phenol)	Predicted SAR effect
1	A — MQIP-H (reduced imine)	Reduce C = N → CH-NH (secondary benzylic amine)	Increased metabolic activity and stability
2	B — MQIP-6F (C6-F on quinoline)	Introducing F at quinoline C6 by SMILES change	Improved bacterial membrane penetration, lipophilicity
3	C — MQIP-N1-cPr (N-alkylation)	N1-cyclopropyl or small alkyl on quinoline nitrogen	Spectrum/potency tuning & membrane passage. Caution should be taken to ensure N-alkylation may change pKa/solubility.
4	D — MQIP, Me→OH (demethylated)	Replace 3-OMe → 3-OH on the o-vanillin ring	Stronger H-bonding & antioxidant activity
5	E — MQIP→oxime (C=N→C=NOH)	Convert azomethine to oxime (C=NOH) at the same position.	Lower hydrolysis, altered H-bonding geometry.
6	F — MQIP-S (o-SH)	Replace ortho-OH → SH (make 2-mercapto-3-MeO benzylidene analog).	Stronger soft-metal affinity (thiolates chelate different metals) and different redox/antibacterial profile
7	G — MQIP→triazole (imine → 1,2,3-triazole linkage)	Replace the C=N–Ar link by a rigid 1,2,3-triazole	Improved metabolic stability and possibly stronger π-stacking for DNA binding

Table 8. DPPH scavenging assay results of MQIP.

Concentration in µg/mL	Blank absorption	Sample absorption	A = $(A_c - A_{TS})/A_c$	% of inhibition = 100 x A
12.5	0.65	0.4845	0.1655	16.55
25	0.65	0.4405	0.2095	20.95
50	0.65	0.3415	0.3085	30.85
100	0.65	0.2125	0.4375	43.75
200	0.65	0.0245	0.6255	62.55
Ascorbic acid IC_{50}	45.35 ± 0.35	**MQIP IC_{50}**		139.83 ± 0.35

applications. SAR of some MQIP related compounds is given in Table 7 below.

4.7. DPPH assay

The antioxidant activity of a compound is tested in vitro by DPPH assay and determining the IC_{50} value of the compound. The IC_{50} equals the effective minimum concentration of the synthesized compound that is required to scavenge about 50% of the free radicals in DPPH assay. A smaller IC_{50} value indicates a stronger antioxidant activity. Specifically, IC_{50} values below 10 mg/mL are often indicative of very robust antioxidant capabilities. Table 8 presents the results of the radical scavenging tests. The % of radical scavenging is obtained by finding the absorption band at 517 nm in the visible range. The results reveal that the level of antioxidant activity improved with increase in electron donating groups in a molecule which generate intramolecular and intermolecular hydrogen bonds. Additionally, the presence of quinoline ring in the chemical further increases its scavenging efficiency. A linear regression graph is drawn and IC_{50} is calculated. The linear regression graph is presented in Figure 10 below. It is found to be 139.83 ± 0.35 µg/mL. From the above antibacterial and antioxidant assay results, it is observed that

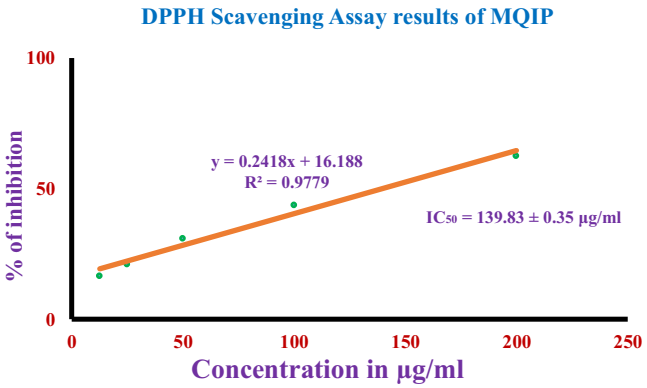

Figure 10. Linear regression graph of the DPPH assay for the R^2 value calculation and performance accuracy identification.

the compound with concentration above 100 µg/mL exhibited efficacy and these results coincidence with the reported results.[53]

4.8. MTT assay of Quinoline Schiff Base MQIP

The colorimetric MTT test is used to assess the in-vitro anticancer activity of MQIP against human breast cancer cell lines

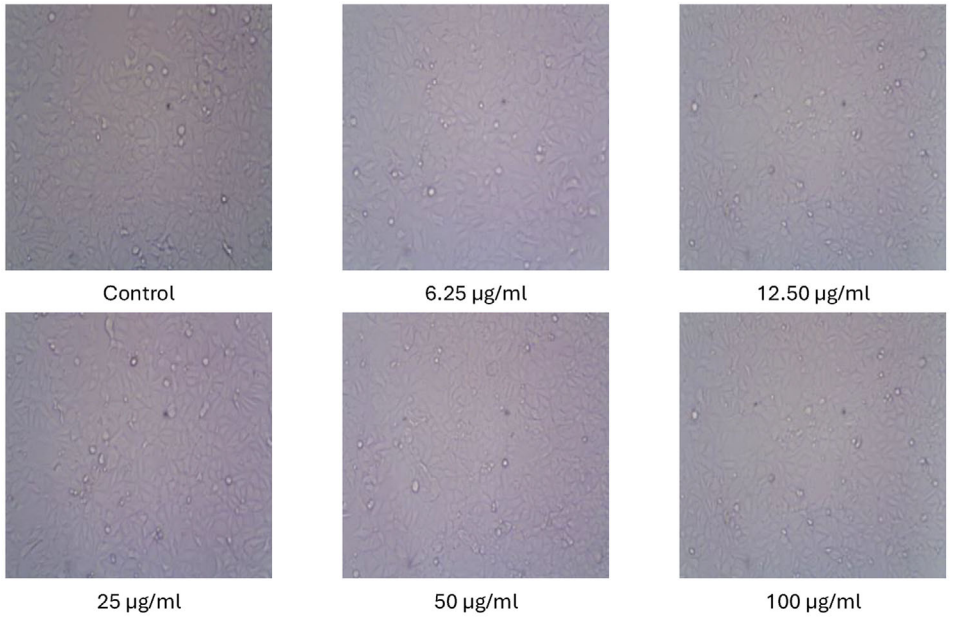

Figure 11. MTT assay of serially diluted concentrations of MQIP against MCF7 cells along with control.

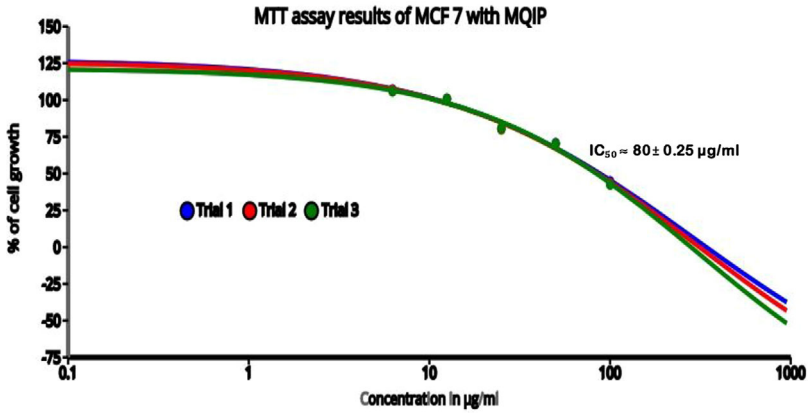

Figure 12. MTT assay outcomes.

(MCF7). The study was conducted with different concentrations of MQIP say 20, 40, 60, 80, and 100 µg/mL in triplicate. In the present experiment, untreated cells were considered as negative control (100% viability) and were incubated with only culture medium + 0.1% DMSO (vehicle). Doxorubicin is taken as positive control – where 10 µg/mL, reduced viability to < 15%, validating assay performance. This is a standard MTT protocol recommended in recent cytotoxicity assays. The culture plates are incubated at 37 °C maintaining 85% humidity and 5% CO_2 for 48 h. After this period, MTT is added and the resulting plates are kept for 3 h after which cell viability is measured. The results of phase-contrast images of MCF-7 cells post-treatment with serially diluted quinoline Schiff base MQIP of different concentration are presented in Figure 11. Experimental results reveal that cell viability was dependent on concentration. A graph of the MTT assay outcomes is shown by Figure 12. The compound exhibited an $IC_{50} \approx 80 \pm 0.25$ µg/ml and the cell growth reduced to 36% for MQIP concentration of 100 µg/mL. This represents good cytotoxic activity of MQIP inherent to the presence of azomethine group with donor atoms of –OH and tertiary nitrogen of quinoline ring.

4.9. Comparison of Literatures

Comparison of the biological activity of various Schiff base compounds reported in literatures is given in Table 9. The results reveal that the synthesized Schiff base MQIP exhibited an antibacterial activity and anticancer activity on-par with the other Schiff bases reported in literature.

Schiff base ligands (L1 to L5) synthesized by condensation of quinoline and aniline were demonstrated to exhibit excellent antioxidant activity with IC_{50} values in the range of (2.29 ± 0.0041 mg/mL) – (22.42 ± 0.0048 mg/mL) in ferric

Table 9. Comparison of MQIP's biological activity.

Ref. No.	Schiff base compound	Antibacterial activity		Anticancer activity (MCF 7)
		ZOI	MIC	IC_{50}
[2]	Bis-Schiff base	8–60 mm	30–61 mg/mL	6.27 ± 0.07 mg/mL
[3]	Schiff base (2,4-dihydroxy benzaldehyde and isobutylamine)	17–19 mm	40 µg/mL	41.5 µg/mL
[54]	Schiff base metal complex	8–38 mm	4–256 µg/mL	–
[55]	Schiff base Sulfadimidines	6–29 mm	1–50 mg/mL	–
[56]	Schiff base (2,4-dihydroxy benzaldehyde 2-amino-3-hydroxy pyridine	–	20 to 55 µg/mL	–
*This work	MQIP	20.4–21.65 mm	12.5 µg/mL	80 ± 0.25 µg/mL

reducing antioxidant power (FRAP) assay.[33] Further, chitosan-Quinoline Schiff base exhibited a quinoline concentration dependent radical scavenging. Specifically, the ligand CHQ was demonstrated to exhibit 59% radical scavenging in ABTS assay.[13] In another experiment, Schiff base ligand was demonstrated to have an IC_{50} value of 138 µg/mL in DPPH assay.[28] Further, studies reveal that metal complexes of Schiff base ligands exhibited improved antioxidant activity in comparison to native ligands.[56] The synthesized MQIP ligand exhibited an IC_{50} value of 139.83 ± 0.35 µg/mL in the DPPH assay. This comparison reveals that the synthesized MQIP ligand demonstrated a good antioxidant activity which is on-par with those reported in literatures [28] and thus, supports the efficacy of the ligand.

5. Conclusion

This work presented a novel Schiff base compound synthesized from the condensation of o-vanillin with Quinoline. Successful formation of the ligand is confirmed by various characterization techniques like UV spectroscopy, FTIR, ^{1}H NMR and ^{13}C NMR. Theoretical QSAR characterisation of the ligand were carried out to confirm its drug likeness. Further, DFT analysis by Spartan-14 enabled understanding its intermolecular interactions and electric property differences. Molecular docking studies of the ligand with various proteins revealed its binding ability with anticancer peptides which supported the anticancer activity of the ligand. These theoretical results are further validated by conducting antibacterial, antioxidant and cell viability assays. Agar-well diffusion assay results revealed that MQIP could inhibit both gram negative and gram-positive bacteria with, (i) ZOI ranging from 20.4 to 21.6 mm and (ii) MIC of 12.6 µg/mL. DPPH assay results revealed that the compound could scavenge ROS with an IC50 value of 139.83 ± 0.35 µg/mL. Further, MTT assay results revealed that the synthesized ligand exhibited anticancer activity against MCF7 breast cancer cells with an IC_{50} value of 80 µg/mL. These results reveal the efficacy of the synthesized ligand and its pharmaceutical potentials. In addition, these capabilities of the ligand kindle further researches in the direction of (i) synthesizing metal complexes from the ligand, (ii) testing its potentials against other cancer cell lines, and (iii) testing its cytotoxicity against normal cell in near future.

Acknowledgments

The authors have nothing to report.

Conflict of Interests

The authors declare no conflict of interest.

Data Availability Statement

The data that support the findings of this study are available from the corresponding author upon reasonable request.

Keywords: Antibacterial · Anticancer activity · Characterization · Docking · Quinoline · Schiff base

[1] A. M. Vargason, A. C. Anselmo, S. Mitragotri, *Nat. Biomed. Eng.* **2021**, *5*, 951–967.
[2] P. Babaei, V. Hadigheh Rezvan, N. Sohrabi Gilani, *Results in Chem.* **2024**, *7*, 101517 https://doi.org/10.1016/j.rechem.2024.101517. (https://www.sciencedirect.com/science/article/pii/S2211715624002133).
[3] A. Arjunan, A. Sebastian, *Future Med. Chem.* **2024**, *16*, 1983–1997.
[4] M. S. More, P. G. Joshi, Y. K. Mishra, P. K. Khanna, *Mater Today Chem.* **2019**, *14*, 100195..
[5] E. Raczuk, B. Dmochowska, J. Samaszko-Fiertek, J. Madaj, *Molecules* **2022**, *27*, 787, https://doi.org/10.3390/molecules27030787.
[6] M. A. El-ghamry, F. M. Elzawawi, A. A. A. Aziz, K. M. Nassir, S. M. Abu-El-Wafa, *Sci. Rep.* **2022**, *12*, 17942.
[7] P. M. Thakor, R. J. Patel, R. K. Giri, S. H. Chaki, A. J. Khimani, Y. H. Vaidya, P. Thakor, A. B. Thakkar, J. D. Patel, *ACS Omega* **2023**, *8*, 33069-33082, https://doi.org/10.1021/acsomega.3c05254.
[8] A. M. Sharma, S. Kishor, S. Mukesh, *J. Chem.* **2009**, *6*, 149837.
[9] H. R. Sonawane, B. T. Vibhute, B. D. Aghav, J. V. Deore, S. K. Patil, *Eur. J. Med. Chem.* **2023**, *258*, 115549, ISSN 0223–5234, https://doi.org/10.1016/j.ejmech.2023.115549. (https://www.sciencedirect.com/science/article/pii/S0223523423005159).
[10] B. Suliphuldevara Matada, R. Pattanashettar, *Bioorg. Med. Chem.* **2021**, *32*, 115973, ISSN 0968-0896, https://doi.org/10.1016/j.bmc.2020.115973. (https://www.sciencedirect.com/science/article/pii/S0968089620308038).
[11] P. Yadav, K. Shah, *Bioorg. Chem.* **2021**, *109*, 104639, ISSN 0045–2068, https://doi.org/10.1016/j.bioorg.2021.104639. (https://www.sciencedirect.com/science/article/pii/S0045206821000158).
[12] L.i-J. Guo, C.-X.i Wei, J.-H. Jia, L.i-M. Zhao, Z.-S. Quan, *Eur. J. Med. Chem.* **2009**, *44*, 954–958, ISSN 0223–5234, https://doi.org/10.1016/j.ejmech.2008.07.010. (https://www.sciencedirect.com/science/article/pii/S0223523408003371).

[13] Y. M. Abdel-Baky, A. M. Omer, E. M. El-Fakharany, Y. A. Ammar, M. S. Abusaif, A. Ragab, *Sci. Rep.* **2023**, *13*, 22792
[14] S. K. Patil, B. T. Vibhute, *Arabian J. Chem.* **2021**, *14* 103285.
[15] M. Gandhi, V. Chavda, S. Ranga, *J. Coord. Chem.* **2025**, *78*, 1303–1336.
[16] S. Satpati, S. K.r. Saha, A. Suhasaria, P. Banerjee, D. Sukul, *RSC Adv.* **2020**, *10*, 9258–9273.
[17] N. Singh, N. Abeer Khan, A. Taha, M. C. Joshi, P. Kumar, A. G. Vedeshwar, *J. Mol. Struct.* **2025**, *1332*, 141722, ISSN 0022–2860, https://doi.org/10.1016/j.molstruc.2025.141722. (https://www.sciencedirect.com/science/article/pii/S0022286025004089).
[18] S. Gurusamy, M. Sankarganesh, N. Revathi, R. Nandini Asha, A. Mathavan, *J. Mol. Liq.* **2023**, *369*, 120941, ISSN 0167–7322, https://doi.org/10.1016/j.molliq.2022.120941. (https://www.sciencedirect.com/science/article/pii/S0167732222024801).
[19] S. T. Tsantis, Z. G. Lada, D. I. Tzimopoulos, V. Bekiari, V. Psycharis, C. P. Raptopoulou, S. P. Perlepes,*Heliyon* **2022**, *8*, e09705, ISSN 2405–8440, https://doi.org/10.1016/j.heliyon.2022.e09705. (https://www.sciencedirect.com/science/article/pii/S2405844022009938).
[20] A. Olatunde, A. Mohammed, M. Auwal Ibrahim, N. Tajuddeen, M. N. Shuaibu, *Eur. J. Med. Chem. Rep.* **2022**, *5*, 100055, ISSN 2772–4174, https://doi.org/10.1016/j.ejmcr.2022.100055. (https://www.sciencedirect.com/science/article/pii/S2772417422000279).
[21] H. L. Singh, N. Dhingra, S. Bhanuka, *J. Mol. Struct.* **2023**, *1287*, 135670, ISSN 0022–2860, https://doi.org/10.1016/j.molstruc.2023.135670. (https://www.sciencedirect.com/science/article/pii/S0022286023007664).
[22] H. Wang, M. Jiang, F. Sun, S. Li, C.-Y. Hse, C. Jin, *MoleculesMolecules* **2018**, *23*, 3027.
[23] Z. Akbari, C. Stagno, N. Iraci, T. Efferth, E. A. Omer, A. Piperno, M. Montazerozohori, M. Feizi-Dehnayebi, N. Micale, *J. Mol. Struct.* **2024**, *1301*, 137400, ISSN 0022–2860, https://doi.org/10.1016/j.molstruc.2023.137400. (https://www.sciencedirect.com/science/article/pii/S0022286023024882).
[24] L. H. Abdel-Rahman, A. A. Abdelghani, A. A. AlObaid, D. A. El-ezz, I. Warad, M. R. Shehata, E. M. Abdalla, *Sci. Rep.* **2023**, *13*, 3199.
[25] M. Bheemarasetti, K. Palakuri, S. Raj, P. Saudagar, D. Gandamalla, N. R. Yellu, L. R. Kotha, *J. Iran. Chem. Soc.* **2018**, *15*, 1377–1389.
[26] G. Venkatesh, P. Vennila, S. Kaya, S. B. Ahmed, P. Sumathi, V. Siva, P. Rajendran, C. Kamal, *ACS Omega* **2024**, *9*, 8123-8138.
[27] S. Shamsian, B. Sokouti, S. Dastmalchi, *Bioimpacts* **2024**, *14*, 29955, https://doi.org/10.34172/bi.2023.29955.
[28] G. K. Ayyadurai, R. Jayaprakash, A. Shajahan, S. Rathika, *J. Biomol. Struct. Dyn.* **2023**, *43*, 2864–2876, https://doi.org/10.1080/07391102.2023.2294383.
[29] L. Touafri; A. Hellal; S. Chafaa; A. Khelifa; A. Kadri, *J. Mol. Struct.* **2017**, *1149*, 750–760, https://doi.org/10.1016/j.molstruc.2017.08.0.
[30] R. Jayaprakash, S. Kumar Sha, S. Hemalatha, D. Easwaramoorthy, *Asian Journal of Pharmaceutical and Clinical Research* **2016**, *9*, 203–8.
[31] M. S. Rana, N. M. A. Rayhan, M. S. H. Emon, M. T. Islam, K. Rathry, M. M. Hasan, M. MM Islam, B. C. Srijon, M. S Islam, A. Ray, M. A. Rakib, A. Islam, M. Kudrat-E-Zahan, M. F. Hossen, M. A. Asraf, *RSC Adv.* **2024**, *14*, 33094-33123, https://doi.org/10.1039/D4RA04375H.
[32] M. Kumar, T. Padmini, K. Ponnuvel, *Journal of Saudi Chemical Society Supplement* **2017**, *21*, S322-S328, ISSN 1319–6103, https://doi.org/10.1016/j.jscs.2014.03.006.
[33] A. A. Adeleke, S. J. Zamisa, M. S. Islam, K. Olofinsan, V. F. Salau, C. Mocktar, B. Omondi, *Antioxidant and Antimicrobial Activities Molecules* **2021**, *26*, 1205.
[34] J.-F. Wang, N. Ren, F.-T. Meng, J.-J. Zhang, *Thermochim. Acta*, **2011**, *512*, 118–123, ISSN 0040–6031, (https://doi.org/10.1016/j.tca.2010.09.011, https://www.sciencedirect.com/science/article/pii/S0040603110003552).
[35] İ. Sıdır, Y. Gülseven Sıdır, S. Góbi, H. Berber, R. Fausto, *MoleculesMolecules* **2021**, *26*, 2814. PMID: 34068634; PMCID: PMC8126046.
[36] M. S. Meenukutty, A. P. Mohan, V. G. Vidya, V. G. Viju Kumar, *Heliyon* **2022**, *8*, e09600, ISSN 2405–8440, https://doi.org/10.1016/j.heliyon.2022.e09600. (https://www.sciencedirect.com/science/article/pii/S240584402200888X).
[37] L. Touafri; A. Hellal; S. Chafaa; A. Khelifa; A. Kadri, *J. Mol. Struct.* **2017**, *1149*, 750–760, https://doi.org/10.1016/j.molstruc.2017.08.0.
[38] M. M. Elsenety; B. A. Elsayed; I. A. Ibrahem; M. A. Bedair, *Inorg. Chem. Commun.* **2020**, *121*, 108213.
[39] B. Vhanale, D. Kadam, A. Shinde, *Heliyon*, **2022**, *8*, e09650, ISSN 2405–8440.
[40] F. Ndidi Ejiah, M. Olarewaju Rofiu, *Mater. Adv.* **2023**, *4*, 2308–2321.
[41] G. Venkatesh, P. Vennila, S. Kaya, S. B. Ahmed, P. Sumathi, V. Siva, P. Rajendran, C. Kamal, *ACS Omega* **2024**, *9*, 8123-8138.
[42] C. A. Lipinski, F. Lombardo, B. W. Dominy, P. J. Feeney, *Adv Drug Deliv Rev* **2001**, *46*, 3-26.
[43] I. M. Vlad; D. C. Nuta; C. Chirita; M. T. Caproiu; C. Draghici; F. Dumitrascu; C. Bleotu; S. Avram; A. M. Udrea; A. V. Missir; L. G. Marutescu; C. Limban, *Molecules* **2020**, *25*, 321.
[44] A. S. Hassan, A. A. Askar, A. M. Naglah, A. A. Almehizia, A. Ragab, *Molecules* **2020**, *25*, 2593.
[45] R. Srivastava, *ACS Omega*. **2021**, *6*, 24891-24901.
[46] I. Mushtaq, M. Ahmad, M. Saleem, A. Ahmed, *Futur J Pharm Sci* **2024**, *10*, 16.
[47] G. Saranya, K. Devendraprasad, P. Shanmugapriya, N. Bhuvaneshwari, *J. Biomol. Struct. Dyn.* **2023**, *41*, 12997-13014..
[48] R. G. Deghadi, A. E. Elsharkawy, A. M. Ashmawy, G. G. Mohamed, *Appl. Organomet. Chem.* **2022**, *36*, e6579, https://doi.org/10.1002/aoc.6579.
[49] C. ; Rachel, K. Monica, *Bioorg. Med. Chem. Lett.* **2020**, *30*, 127655.
[50] A. M. Asiri; S. A. Khan, *Molecules* **2010**, *15*, 6850–6858.
[51] Y. D. Bodke; S. Shankerrao; R. Kenchappa; S. Telkar, *Russ. J. Gen. Chem.* **2017**, *87* 1843–1849.
[52] B. K. Mallandur, G. Rangaiah, N. V. Harohally, *Synth. Commun.* **2017**, *47* 1065–1070.
[53] Y.e Zhang; Y. Fang; H. Liang; H. Wang; K. Hu; X. Liu; X. Yi; Y. Peng, *Bioorg. Med. Chem. Lett.* **2013**, *23* 107–111.
[54] S. K. Zabiulla, M. Joythi, A. Bushra Begum, M. S. Asha, F. H. Al-Ostoot, D. P. Lakshmeesha, R. Ramu, *Results in Chem.* **2023**, *5*, 100650, ISSN 2211–7156, https://doi.org/10.1016/j.rechem.2022.100650. (https://www.sciencedirect.com/science/article/pii/S2211715622003691).
[55] H. H. Amer, E. H. Eldrehmy, S. M. Abdel-Hafez, Y. S. Alghamdi, M. Y. Hassan, S. H. Alotaibi, *Sci Rep.* **2021**, *11*, 17953, https://doi.org/10.1038/s41598-021-97297-1.
[56] A. Z. El-Sonbati, A. A. El-Bindary, N. M. Mansour, M. M. El-Zahed, *BMC Chem.* **2025**, *19*, 177, https://doi.org/10.1186/s13065-025-01561-8.

Manuscript received: July 14, 2025